 doi:10.20944/preprints202204.0038.v1

Thermodynamics and the Goldman-Hodgkin-Katz equation

Hirohisa Tamagawa* · **Toi Nakahata** · **Ren Sugimori** · **Bernard Delalande**

Abstract Current physiology attributes the mechanism of membrane potential generation to transmembrane ion transport, but ion adsorption could just as well play this fundamental role. The evidence shows that the ion adsorption mechanism accurately reproduces the experimentally measured membrane potential. The Goldman-Hodgkin-Katz equation (GHK eq.) and the Nernst equation (Nernst eq.) are the typical mathematical formulas representing the membrane potential in current physiology. However, the authors were able to show that the potential formulas by ion adsorption mechanism give identical results to GHK eq. and Nernst. eq. Our experimental and theoretical analyses suggest that there is a special relationship between the membrane potential and the membrane surface charge density, and this unique equation inevitably leads to the establishment of a GHK eq and/or a Nernst eq. The authors found that the unique equation is the foundation of thermodynamics "Boltzmann distribution". Thus, the GHK eq. and the Nernst eq. are simply the natural consequence of thermodynamics from the view of the ion adsorption mechanism.

Keywords Goldman-Hodgkin-Katz eq.; Nernst eq.; ion adsorption; membrane potential

H. Tamagawa*,†1, T. Nakahata†2, R. Sugimori†3
Department of Mechanical Engineering, Faculty of Engineering, Gifu University, 1-1 Yanagido, Gifu, Gifu, 501-1193 Japan
Tel.: +81-58-293-2529
Fax: +81-58-293-2529
E-mail: tmgwhrhs@gifu-u.ac.jp†1, http://orcid.org/0000-0003-0532-8278;
y3031086@edu.gifu-u.ac.jp†2; eyemask2000@gmail.com†3
*: Corresponding author

B. Delalande
280 avenue de la Pierre Dourdant, 38290 La Verpilliere, France
E-mail: bernard@somasimple.com, http://orcid.org/0000-0003-2451-2791

Preprints (www.preprints.org) | NOT PEER-REVIEWED | Posted: 6 April 2022 doi:10.20944/preprints202204.0038.v1

1 Introduction

The Goldman-Hodgkin-Katz equation (GHK eq.) has played a central role in electrophysiology to this day [1–5], and can quantitatively and accurately predict a membrane potential [6–8]. The basis of the GHK equation is the assumption that continuous transmembrane ion transport governs the characteristics of the membrane potential.

In 2018, new interpretations of GHK eq. were provided by Tamagawa and Ikeda [9,10]. They measured the potential generated through an impermeable silver wire coated with $AgCl$ between two electrolyte solutions. One solution was composed of KCl & KBr, while the other was made up of KCl. Tamagawa and Ikeda derived the formula for the potential of this system is given by Eq. 1 by attributing the origin of the potential to ions adsorption. Thus, K_i in the Eq. 1 represents the binding constant between an ion (Cl^-, Br^-) and its adsorption site on the surface of $AgCl$. Intriguingly enough, the GHK eq., Eq. 2 is identical to Eq. 1 if the GHK eq. is applicable to this system. Namely, replacing P_i, which represents the permeability constant of separator ($AgCl$-coated silver wire in this case) to the mobile ion i, by K_i results in Eq. 1. Therefore, Eq. 1 is identical to Eq. 2 although the assumptions necessary for the use of these two equations are completely different from each other. Tamagawa and Ikeda emphasized that the membrane potential must be governed by the ion adsorption as represented by Eq. 1 and questioned the traditionally accepted basis of the GHK eq, namely that the membrane potential is governed by transmembrane ion transport.

$$\phi^{ADS} = -\frac{kT}{e} \ln \frac{K_{Cl}[Cl]_R}{K_{Cl}[Cl]_L + K_{Br}[Br]_L} \tag{1}$$

$$\phi^{GHK} = -\frac{kT}{e} \ln \frac{P_{Cl}[Cl]_R}{P_{Cl}[Cl]_L + P_{Br}[Br]_L} \tag{2}$$

The authors of this paper have recently re-examined the membrane potential from the point of view of the ion adsorption mechanism and found that there appears to be an intimate correlation between the potential generated and the charge density on the separator surface. It seems to lead inevitably to the GHK eq. and/or the Nernst eq. (the Nernst eq. is the simpler version of the GHK eq. [6–8]). Namely, the expression of the potential formula identical to GHK eq. and Nernst eq. is the naturally derived consequence of the analysis of the membrane potential based on the ion adsorption mechanism.

In this paper, the authors will present the reasons why the GHK eq. and the Nernst eq. are the natural consequences of the membrane potential generation mechanism.

2 Previous works

2.1 Potential across the $AgCl$-coated silver wire

Ion adsorption-based membrane potential generation mechanism was reported by Tamagawa and Ikeda in 2018 [9,10]. The basis of this mechanism was formed by the

Preprints (www.preprints.org) | NOT PEER-REVIEWED | Posted: 6 April 2022 doi:10.20944/preprints202204.0038.v1

late Chinese-American physiologist, Gilbert N. Ling. Although he is best known for his development of the $Ag/AgCl$ electrode, which has been widely used in electrophysiology to this day, his most important achievement was the creation of his own physiological concept called the Association-Induction Hypothesis (AIH) [11–14]. However, the AIH is in conflict with the prevailing physiological concept and has therefore ousted Ling from the scientific community despite his monumental achievement, the creation and perfection of a practical Ag/AgCl electrode. Only a handful of research groups have continued to work in this and related fields of physiology, siding with the AIH. [13–20].

First, the work of Tamagawa and Ikeda in refs.[9,10] is briefly explained in a simplified manner as below. They measured the potential across the $AgCl$-coated silver wire between two electrolyte solutions, one consisting of KCl & KBr, the other of KCl, as shown in the Fig. 1. The key to their work is that the $AgCl$-coated silver wire they used was non-permeable. However, the experimental potential data was found to be quantitatively reproducible by the GHK eq. (Eq. 2) using hypothetical permeability coefficients P_i.

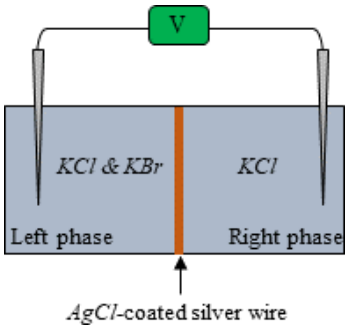

Fig. 1 A fundamental facet of the experimental set-up used in the Tamagawa and Ikeda's experiment in the ref. [9]. Caution: The illustration represents the essential part of the installation but does not represent its details exactly or precisely.

Tamagawa and Ikeda studied the characteristics of the experimentally measured potential in terms of the ion adsorption mechanism. They hypothesized that Cl^- and Br^- are adsorbed on the surfaces of $AgCl$-coated silver wire. The surface charge density depends on the amount of adsorbed ions. Figure 2 represents the expected potential profiles. The characteristics of the left phase potential are governed by the experimental condition of the left phase only but have nothing to do with the condition of the right phase. The same applies to the characteristics of the right-hand phase potential. In other words, the potential profiles of the two phases are determined independently each other. Tamagawa and Ikeda computed the expected potential profile in the left phase by deriving the well-known Poisson-Boltzmann equation (PB eq.) [21–23]. The expected right phase potential profile was derived in the same way. Tamagawa and Ikeda successfully derived the formula of the $AgCl$ surface potential represented by ϕ_L^{ADS} and ϕ_R^{ADS} shown in Fig. 2. By plugging those ϕ_L^{ADS} and ϕ_R^{ADS} into Eq. 3, Eq. 1 was derived. The exact process is described in the ref. [9]. As mentioned earlier, Eq. 1 is identical to

Preprints (www.preprints.org) | NOT PEER-REVIEWED | Posted: 6 April 2022 doi:10.20944/preprints202204.0038.v1

the GHK eq., Eq. 2. As a result, a doubt has arisen as to the validity of the GHK eq. per se.

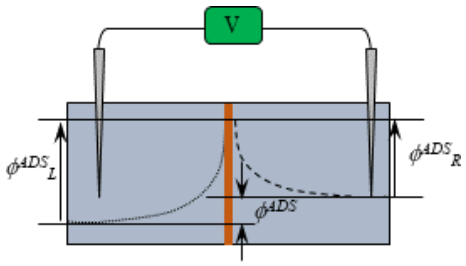

Fig. 2 Expected potential profiles represented by the dotted and dashed lines

$$\phi^{ADS} = (-\phi_L^{ADS}) - (-\phi_R^{ADS}) \tag{3}$$

In the process of deriving Eq 1, Tamagawa and Ikeda developed Eqs. 4 and 5 as detailed in the ref. [9] (see the notation table Table 1). Both give the surface charge density, $\sigma|_{x=0}$, of $AgCl$-coated silver wire surface. Eq. 4 is not a special equation at all, but it is very common and can be found even in ordinary textbooks. The Eq. 5 has been derived using ordinary physical chemistry [24].

$$\sigma|_{x=0} = 2\sqrt{\epsilon\epsilon_0 Q_\infty kT}\sinh(\beta\phi_0) \tag{4}$$

$$\sigma|_{x=0} = \sigma_o - e[s]_T \frac{(K_{Cl}Q_{Cl} + K_{Br}Q_{Br})exp(2\beta\phi_0)}{1 + (K_{Cl}Q_{Cl} + K_{Br}Q_{Br})exp(2\beta\phi_0)} \tag{5}$$

Table 1 Notations

ϵ	relative permittivity of water	80
ϵ_0	vacuum permittivity	$8.85\times\ 10^{-12}$ / Fm^{-1}
e	elementary charge	$1.60\times\ 10^{-19}$ / C
k	Boltzmann constant	$1.38\times\ 10^{-23}$ / m^2kgs^{-2}
T	temperature	298 / K
Q_i	bulk phase concentration of i	$i = Cl^-, Br^-$
Q_∞	total bulk phase anion concentration	$Q_\infty \equiv Q_{Cl} + Q_{Br}$
K_i	binding constant between i and s	$K_i \equiv [si]/[s][i]\|_{x=0}$
$\sigma\|_{x=0}$	separator surface charge density	
ϕ_0	$AgCl$ surface potential	
σ_o	$AgCl$-coated silver wire surface charge density without ion adsorption	
s	surface adsorption site for the mobile anions i ($i = Cl^-, Br^-$)	
$[s]_T$	total ion adsorption site density of the separator surface	
β	$\beta \equiv e/2kT$	

Tamagawa and Ikeda found that inserting the experimental data of Q_∞ and ϕ_0 into Eq. 4 resulted in the fact that somehow the surface charge density of the

Preprints (www.preprints.org) | NOT PEER-REVIEWED | Posted: 6 April 2022 doi:10.20944/preprints202204.0038.v1

AgCl-coated silver wire, $\sigma|_{x=0}$, is kept almost constant as indicated by Eq. 6. Therefore, Eq. 5 is held nearly constant, too, as represented by Eq. 7.

$$\sigma|_{x=0} \sim const. \tag{6}$$

$$const. \sim \sigma_o - e[s]_T \frac{(K_{Cl}Q_{Cl} + K_{Br}Q_{Br})exp(2\beta\phi_0)}{1 + (K_{Cl}Q_{Cl} + K_{Br}Q_{Br})exp(2\beta\phi_0)} \tag{7}$$

Solving Eq. 7 with respect to ϕ_0 gives Eq.8. Applying Eq. 8 to the left-hand phase of the experimental system in Fig. 2 gives the Eq. 9. The same applies to the right-hand phase.

$$\phi_0 \sim \frac{kT}{e} \ln \frac{A}{K_{Cl}Q_{Cl} + K_{Br}Q_{Br}} \quad A \equiv const. \tag{8}$$

$$\phi_L^{ADS} = -\phi_0(\text{L(eft) phase}) \sim -\frac{kT}{e} \ln \frac{A}{K_{Cl}Q_{Cl}^L + K_{Br}Q_{Br}^L} \tag{9}$$

By incorporating Eq. 9 into Eq. 3, we obtain ϕ^{ADS} as given by Eq. 10 (identical to Eq. 1). Therefore, the analysis based on ioni adsorption gives a potential formula identical to the GHK eq.

$$\begin{aligned} \phi^{ADS} &= \phi_L^{ADS} - \phi_R^{ADS} \\ &\sim \left(-\frac{kT}{e} \ln \frac{A}{K_{Cl}Q_{Cl}^L + K_{Br}Q_{Br}^L}\right) - \left(-\frac{kT}{e} \ln \frac{A}{K_{Cl}Q_{Cl}^R + K_{Br}Q_{Br}^R}\right) \\ &= -\frac{kT}{e} \ln \frac{K_{Cl}Q_{Cl}^R}{K_{Cl}Q_{Cl}^L + K_{Br}Q_{Br}^L} \quad \because [Br^-]_R = 0 \end{aligned} \tag{10}$$

Considering the procedure described so far, the key to obtaining Eq. 10 is the experimental finding Eq. 6. In other words, Eq. 4 is constant. It can be simplified to Eq. 11.

$$\sqrt{Q_\infty} \sinh(\beta\phi_0) \sim const. \tag{11}$$

Before continuing the discussion on Eq. 11, the authors wish to move on to the next step described in the next section and then return to Eq. 11 in the section **3. Keys for the establishment of GHK eq. and Nernst eq.**

2.2 Potential across the lithium glass

2.2.1 Derivation of the potential formula

The authors carried out the other measurement of the potential across the lithium glass between two electrolyte solutions using the same set-up illustrated in Fig 3. The $AgCl$-ted silver wire was replaced by the lithium glass plate (LICGC^{TM}PW-01, OHARA INC., Kanagawa, Japan), and the left-hand solution was a $LiCl$ solution while the right-hand solution was a KCl solution. The potential measurement was performed by varying the concentration of $LiCl$ while maintaining the concentration of KCl.

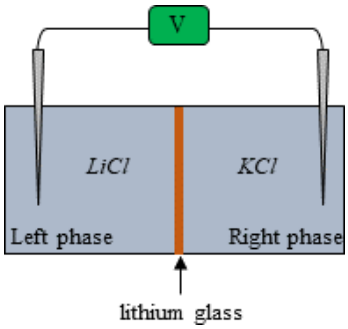

Fig. 3 The experimental setup for measuring the potential generated across the lithium glass between the left $LiCl$ solution and the right KCl solution

Figure 4 shows the experimentally measured potential profiles. This experimental result indicates that the potential is sensitive to the amount of Li^+ but indifferent to KCl since the 100-fold difference in $[KCl]$ in the right phase caused almost no change in potential. It means that $LiCl$ potential is indifferent to KCl quantity. The authors assumed that the potential profile could be approximated by the dashed and dotted curves shown in Fig. 5. The potential measured by the authors corresponds to V^{ADS} in Fig. 5. The important thing about this potential profile is that the potential profile of the right phase represented by the dotted line is flat. Thus, the potential of the right surface of the lithium glass v_R^{ADS} is practically zero. Therefore, the experimentally measured potential V^{ADS} can be considered as the potential of the left surface of the lithium glass v_L^{ADS}. It is represented by Eq.12. Consequently, the surface potentials of the lithium glass in contact with the $LiCl$ solution of concentration Q_∞ are abstracted in Table 2.

$$v_L^{ADS} = V^{ADS} \tag{12}$$

The authors hypothesized that Li^+ is adsorbed on the left surface of the lithium glass and then attempted to theoretically derive the formula for the left surface potential of the lithium glass using essentially the same manner described in the previous section. Eq. 13 was obtained. The derivation process is described in **Appendix A**.

Preprints (www.preprints.org) | NOT PEER-REVIEWED | Posted: 6 April 2022 doi:10.20944/preprints202204.0038.v1

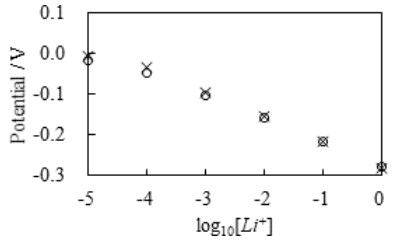

Fig. 4 Potential across the lithium glass against the left phase $[Li^+]$ ◯: when $[KCl]$ in the right phase is 0.0001M ×: when $[KCl]$ in the right phase is 0.01M

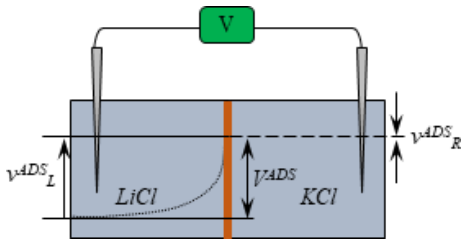

Fig. 5 Expected potential profiles represented by the dotted (Left phase potential profile) and dashed (Right phase potential profile) lines

Table 2 Surface potential of lithium glass

Q_∞†1 / M	ϕ_0†2 / V
0.00001	0.0182
0.0001	0.0484
0.001	0.1022
0.01	0.1588
0.1	0.2166
1.0	0.2784

†1 Bulk phase concentration of Li^+ in the left phase of setup illustrated in Fig. 5
†2 ϕ_0 corresponds to v_L^{ADS} in Fig. 5 under the condition given by Eq. 12.

$$\phi_0(\mathrm{L(eft)\ phase}) \sim N + \frac{kT}{e} \ln Q_\infty^L \equiv \Phi_L^{ADS} \tag{13}$$

If the left and right solutions of the setup in Fig. 3 are solutions of $LiCl$ as shown in Fig. 6, the right surface potential of lithium glass is given by the Eq. 14. Then the potential across the lithium glass can be given by Eq. 15, resulting in Eq. 16 by using Eqs. 13 and 14. Eq. 16 is the same expression as the Nernst eq. [6–8,11,24]. Thus, the equation widely used in physiology, the Nernst eq., is derived using the ion adsorption mechanism. Nernst eq. can be regarded as the simplest version of GHK eq. [6–8].

$$\phi_0(\mathrm{R(ight)\ phase}) \sim N + \frac{kT}{e} \ln Q_\infty^R \equiv \Phi_R^{ADS} \tag{14}$$

Preprints (www.preprints.org) | NOT PEER-REVIEWED | Posted: 6 April 2022 doi:10.20944/preprints202204.0038.v1

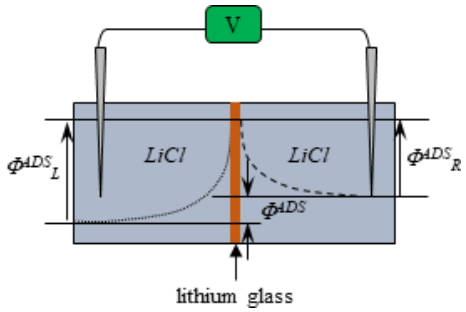

Fig. 6 Experimental set-up when using lithium glass and two $LiCl$ solutions.

$$\Phi^{ADS} = (-\Phi_L^{ADS}) - (-\Phi_R^{ADS}) \tag{15}$$

$$\Phi^{ADS} = -\frac{kT}{e} \ln\left(\frac{Q_\infty^L}{Q_\infty^R}\right) (\equiv \Phi^{Nernst}) \tag{16}$$

The author checked experimentally whether the potential across the lithium glass occurring between two $LiCl$ solutions could be reproduced using Eq. 16 in the next section.

2.2.2 Verification of the potential formula

Prior to proceeding with the verification of Eq. 16, the authors experimentally measured the potential between two $LiCl$ solutions separated by a lithium glass using the setup shown in Fig. 6. The concentration of $LiCl$ in the left phase was varied from 0.00001M to 1M while the concentration of $LiCl$ in the right phase was maintained at 0.0001M. The results are shown in Table 3 as Φ^{EXP}. Then, the author computed the potential using Eq. 15. The experimental surface potential data presented in Table 2 are inserted into Eq. 15, resulting in the data presented in the third column of Table 3. Thus, the results of the Eq. 15 are in good agreement with the directly measured potential generated through the lithium glass given by Φ^{EXP}. In addition, the author has computed using Eq. 16. Plugging the bulk phase ionic concentration data Q_∞^L (0.00001M $\sim$ 1M) and Q_∞^R (= 0.0001M) into Eq. 16 gives the computed potential Φ^{Nernst} shown in the fourth column of Table 3. Φ^{Nernst} is also in the quite good agreement with Φ^{EXP} and Φ^{ADS}. Φ^{EXP}, Φ^{ADS} and Φ^{Nernt} are summarized in Fig. 7. So, Φ^{ADS} is derived by the ion adsorption mechanism and it can reproduce the experimental data of Φ^{EXP}. Furthermore, the expression of formula Φ^{ADS} can lead to the expression of Φ^{Nersnt}. Therefore, the ion adsorption mechanism is reliable enough as a mechanism for generating the membrane potential. It must be worthy enough to investigate the reason for the establishment of Eq. 16.

The key for reaching Eqs. 14 $\sim$ 16 is Eq. A.20 in **Appendix A**. Eq. A.20 can be further arranged into Eq. 17.

Preprints (www.preprints.org) | NOT PEER-REVIEWED | Posted: 6 April 2022 doi:10.20944/preprints202204.0038.v1

Table 3 Potential across the lithium glass

Q_∞ / M	Φ^{EXP}†1	Φ^{ADS}†2 / V	Φ^{Nernst}†3 / V
0.00001	0.027	0.030	0.059
0.0001	0.007	0.000	0.000
0.001	-0.048	-0.054	-0.059
0.01	-0.102	-0.110	-0.118
0.1	-0.163	-0.168	-0.177
1.0	-0.231	-0.230	-0.237

†1 Φ^{EXP} is experimentally measured potential generated across the lithium glass intervening two KCl solutions where the Right phase $LiCl$ concentration is maintained constant 0.0001 M.
†2 Φ^{ADS} is computed by plugging the experimental surface potential shown in Table 2 into both LHS and RHS of Eq. 15
†3 Φ^{Nernst} is computed by plugging the experimental bulk phase $[Li^+]$ data into Eq. 16

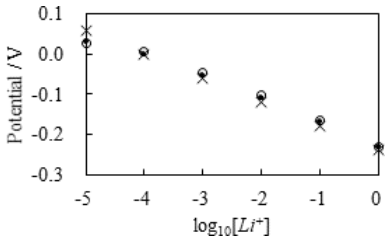

Fig. 7 Φ^{EXP} (◯), Φ^{ADS} (●) and Φ^{Nernt} (×) against the Left phase $\log_{10}[Li^+]$

$$\frac{1}{\sqrt{Q_\infty}}\sinh(\beta\phi_0) \sim const. \tag{17}$$

3 Keys for the establishment of GHK eq. and Nernst eq.

3.1 The key equation from the view of ion adsorption mechanism

Eq. 17 is a key to reach the Nernst type equation of Eq. 16. Eq.11 presented previously is also the key equation to reach the GHK type equation of Eq.10. The two equations Eq. 10 and 17 are very similar. Eqs. 10 and 17 suggest that the surface potential ϕ_0 is generated in such a way that either Eqs. 10 or 17 hold, although the authors have not elucidated why (but the authors will show our view to this in the next section 3.2. The ground for the key equation). Conversely, either 10 or 17 must hold for the establishment of GHK and/or Nernst type equations as long as the mechanism of generation of the membrane potential is attributed to the ion adsorption phenomenon. So, the ion adsorption mechanism may truly play the fundamental role for generating the membrane potential though the current physiology attributes the generation mechanism of membrane potential to the transmembrane ion transport. Eq. 10 is for the system involving the anion adsorption while Eq. 17 is for the system the cation adsorption is involved. Hence, both equations must be unified as a single equation Eq. 18.

Preprints (www.preprints.org) | NOT PEER-REVIEWED | Posted: 6 April 2022 doi:10.20944/preprints202204.0038.v1

$$Q_{\infty}^{-z_i/2}\sinh(\beta\phi_0) = const. \quad z_i = \text{valency of the adsorbed ion} \tag{18}$$

The ion adsorption mechanism seems to lead inevitably to the GHK eq. If this is really the case, then the GHK eq. and the Nernst eq. in biology are only the natural consequence of the emergence of ions from the ion adsorption mechanism.

3.2 The ground for the key equation

Eq. 18 is scrutinized here. When z_i is +1, Eq. 17 is derived from Eq. 18. Eq. 17 is originally the RHS of Eq. A.19 in **Appendix A**. Since the experimental observations validate Eqs. A.20 and A.21, Eq. 20 is attained.

$$\text{RHS of Eq. A.19} = 2\sqrt{\frac{2\epsilon\epsilon_o kT}{Q_{\infty}}}\sinh(\beta\phi_0) \tag{19}$$

Solving Eq. 20 with respect to ϕ_0 leads to Eq. 21. Following the procedure described in the section 2.2.1. Verification of the potential formula using Eq. 21, the Nernst eq. of Eq. 22 is derived.

$$\sqrt{\frac{2\epsilon\epsilon_o kT}{Q_{\infty}}}\exp(\beta\phi_0) \sim const. \tag{20}$$

$$\phi_0 \sim N + \frac{kT}{e}\ln Q_{\infty} (= \text{Eqs. 13 and 14}) \tag{21}$$

$$\Phi^{ADS} = -\frac{kT}{e}\ln\left(\frac{Q_{\infty}^{L}}{Q_{\infty}^{R}}\right) (= \text{Eq. 16}) \tag{22}$$

Now, the authors will analyze Eq. 16. Eq. 16 is Nernst eq., and it is fully validated as one of fundamental equations in physical chemistry [24]. Therefore, Eq. 22 has be scientifically valid apart from the work described in this paper. So, let's forget the discussion so far made and let's focus on the Nernst eq. from the clean slate.

Eq. 16 can be transformed in to Eq. 23 by introducing V_L and V_R defined by Eq. 24. LHS of Eq. 23 is identical to RHS of Eq. 23, and at the same time the LHS is governed only by the physical quantity of the Left phase of the system in question, while the RHS is governed by the physical quantity of the Right phase only. Hence, both sides of Eq. 23 leads to Eq. 25. If V^i is redenoted by " $-\Phi_j^{ADS}$ " $(j = L, R)$ and "const" of Eq. 25 is redenoted by "$-N$", Eqs. 26 and 27 are derived.

$$V^L + \frac{kT}{e}\ln(Q_{\infty}^{L}) = V^R + \frac{kT}{e}\ln(Q_{\infty}^{R}) \tag{23}$$

Preprints (www.preprints.org) | NOT PEER-REVIEWED | Posted: 6 April 2022 doi:10.20944/preprints202204.0038.v1

$$\Phi^{ADS} = V^L - V_R \tag{24}$$

$$V^L + \frac{kT}{e}\ln(Q_\infty^L) = V^R + \frac{kT}{e}\ln(Q_\infty^R) = const. \tag{25}$$

$$\Phi_L^{ADS}(= -V^L) = N + \frac{kT}{e}\ln(Q_\infty^L) \tag{26}$$

$$\Phi_R^{ADS}(= -V^R) = N + \frac{kT}{e}\ln(Q_\infty^R) \tag{27}$$

Eqs. 26 and 27 are Eqs. 13 and 14, respectively. So, Eqs. 13 and 14 are in fact the natural consequences derived from the widely-known Nernst eq. Therefore, there is nothing strange in the ion adsorption mechanism as the cause of membrane potential generation. Further, these two equations can be rearranged into Eq. 28.

$$\begin{aligned} & \Phi_j^{ADS} = N + \frac{kT}{e}\ln(Q_\infty^j) \\ \rightleftharpoons \quad & \exp\left(-\frac{eN}{kT}\right) = Q_\infty^j \exp\left(-\frac{e\Phi_j^{ADS}}{kT}\right) \quad (j = L, R) \end{aligned} \tag{28}$$

RHS of Eq. 28 means the ion distribution obeying Boltzmann distribution. Therefore, LHS represents the ion concentration at the position where the potential is Φ_j^{ADS}. Moreover, LHS "should" be the ion concentration at the position where the potential is Φ_j^{ADS}, otherwise, Eq. 28 cannot have the thermodynamical meaning. Eq. 28 is derived from the well-known thermodynamical equation, Nernst eq. of Eq. 22. Therefore, the LHS should be interpreted as the ion concentration at the position where the potential is Φ_j^{ADS}.

Eq. 11 could be interpreted thermodynamically in the same way as Eq. 17 is interpreted in this section (see **Appendix B**, too), and it could lead to one equation which is identical to GHK eq. like Eq. 1. So, both GHK eq. and Nersnt eq. must be merely another mathematical expressions of Boltzmann distribution of ions which are derivable by attributing the membrane potential generation mechanism to the ion adsorption rather than to the transmembrane ion transport.

4 Conclusion

This work suggests that the GHK eq. and the Nersnt eq., which are widely used in current physiology for quantitative analysis of the membrane potential, can be derived even by attributing the mechanism of membrane potential generation to ion adsorption, although current physiology attributes the generation of the membrane potential to the occurrence of continuous transmembrane ion transport. The authors found that there appears to be a a particular relationship between the surface potential of the separator and its surface charge density, as given by

the Eq. 18, and the Eq. 18 leads inevitably to the establishment of the GHK eq. and the Nernst eq. Although Eq. 18 might be established simply by coincidence, the authors theoretically and thermodynamically suggest that GHK eq. and the Nersnt eq. could be merely another mathematical expressions of Boltzmann distribution which a re derivable by viewing the membrane potential as an electrical consequence of ion adsorption.

Declaration of COI: The author states that there is no conflict of interest.

References

1. Peter H. Barry. *The Reliability of Relative AnionCation Permeabilities Deduced From Reversal (Dilution) Potential Measurements in Ion Channel Studies.* Cell Biochemistry and Biophysics, 46:143–154, 2006.
2. John R. Clay, David Paydarfar, Daniel B. Forger. *A simple modification of the Hodgkin and Huxley equations explains type 3 excitability in squid giant axons.* J. R. Soc. Interface, 5:1421–1428, 2009. doi:10.1098/rsif.2008.0166.
3. John R. Clay. *Determining K^+ channel activation curves from K^+ channel currents often requires the GoldmanHodgkinKatz equation.* Frontiers in CELLULAR NEUROSCIENCE, 3:1–6, 2009. doi: 10.3389/neuro.03.020.2009.
4. Casandra M. Monzon, Rossana Occhipinti, Omar P. Pignataro, Jeffrey L. Garvin. *Nitric oxide reduces paracellular resistance in rat thick ascending limbs by increasing Na^+ and Cl^- permeabilities.* Am. J. Physiol. Renal Physiol., 312:F1035–F1043, 2017. doi:10.1152/ajprenal.00671.2016.
5. Carlos Navarro-Retamal, Stephan Schott-Verdugo, Holger Gohlke, Ingo Dreyer. *Computational Analyses of the AtTPC1 (Arabidopsis Two-Pore Channel 1) Permeation Pathway.* Int. J. Mol. Sci., 22:10345, 2021.
6. J. Cronin. *Mathematical Aspects of Hodgkin-Huxley Neural Theory.* Cambridge University Press, New York, 1987.
7. James Keener, James Sneyd. *Mathematical Physiology: I: Cellular Physiology (Interdisciplinary Applied Mathematics).* Springer, 2008.
8. G. Bard Ermentrout, David H. Terman. *Mathematical Foundations of Neuroscience (Interdisciplinary Applied Mathematics Book 35).* Springer, New York, 2010.
9. H. Tamagawa, K. Ikeda. *Another interpretation of Goldman-Hodgkin-Katz equation based on the Ling's adsorption theory.* Eur. Biophys. J., 47:869–879, 2018.
10. H. Tamagawa. *Mathematical expression of membrane potential based on Lings adsorption theory is approximately the same as the GoldmanHodgkinKatz equation.* J. Biol. Phys., 45:13–30, 2018.
11. Gilbert N. Ling. *A Revolution in the Physiology of the Living Cell.* Krieger Pub Co, Malabar, Florida, 1992.
12. Gilbert N. Ling. *Life at the Cell and Below-Cell Level: The Hidden History of a Fundamental Revolution in Biology.* Pacific Press, New York, 2001.
13. Gerald H. Pollack. *Cells, Gels and the Engines of Life: A New, Unifying Approach to Cell Function.* Ebner & Sons, Seattle, USA, 2001.
14. Gerald H. Pollack. *The Fourth Phase of Water: Beyond Solid, Liquid, and Vapor.* Ebner & Sons, Seattle, USA, 2014.
15. Daniel C. Elton, Peter D. Spencer, James D. Riches, Elizabeth D. Williams. *Potassium adsorption sites in frog muscle visualized by cesium and thallium under transmission electron microscope.* Physiol. Chem. Phys., 9(4/ 5):313–317, 1977.
16. Daniel C. Elton, Peter D. Spencer, James D. Riches, Elizabeth D. Williams. *Preferential localized uptake of K^+ and Cs^+ over Na^+ in the A-band of freeze-dried embedded muscle section - detection by x-ray-micro-analysis and laser micro-probe mass analysis.* Physiol. Chem. Phys., 12(6):509–514, 1980.
17. Gary E. Wnek. *Perspective: Do Macromolecules Play a Role in the Mechanisms of Nerve Stimulation and Nervous Transmission?* JOURNAL OF POLYMER SCIENCE, PART B: POLYMER PHYSICS, 54:7–14, 2015.

18. Matthias F. Schneider. *Living systems approached from physical principles.* Progress in Biophysics and Molecular Biology, 162:2–25, 2021. https://doi.org/10.1016/j.pbiomolbio.2020.10.001.
19. Luis A. Bagatolli, Roberto P. Stock. *Lipids, membranes, colloids and cells: A long view.* BBA - Biomembranes, 1863, Paper No. 183684, 2021. doi.org/10.1016/j.bbamem.2021.183684.
20. Luis A. Bagatolli, Agustn Mangiarotti, Roberto P. Stock. *Cellular metabolism and colloids: Realistically linking physiology and biological physical chemistry.* Progress in Biophysics and Molecular Biology, 162:79–88, 2021. doi.org/10.1016/j.pbiomolbio.2020.06.002.
21. A. Kitahara, A. Watanabe. *Surfactant Science Series Volume 15, Electrical Phenomena at Interface Fundamentals, Measurements, and Applications.* Dekker: New York, NY, USA, 1984.
22. J. OM. Bockris. *Surface Electrochemistry: A Molecular Level Approach.* Springer: New York, NY, US, 1993.
23. C. M. A. Brett, A. M. O. Brett. *Electrochemistry Principles, Methods and Applications.* Oxford University Press: New York, NY, USA, 1993.
24. Gordon M. Barrow. *Physical Chemistry.* McGraw-Hill Inc., 1984.

Appendix A

Assuming that an s represents an adsorption site on the lithium glass surface for a Li^+, the chemical equilibrium represented by the Eq. A.1 is derived. By denoting the binding constant between s and Li^+ by K_{Li}, Eq. A.2 is obtained by the law of mass action.

$$Li^+ + s \rightleftharpoons sLi^+ \tag{A.1}$$

$$K_{Li} = \frac{[si]}{[s][Li^+]|_{x=0}} \tag{A.2}$$

Figure A.1 shows the configuration illustrated in Fig. 3 with the coordinate system. In the left-hand phase of Fig. A.1, the ion concentrations are given by Eqs. A.3 and A.4, respectively, under the condition Eq. A.5 where Q_{Li} and Q_{Cl} represent the bulk phase concentration of K^+ and Cl^-, respectively, and ϕ represents the potential. Eqs. A.3 and A.4 merely represent the ion Boltzmann distribution. Namely, they are so called Poisson-Boltzmann equation (PB eq.) [24].

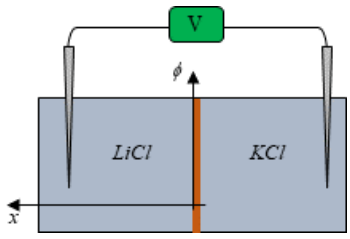

Fig. A.1 The experimental setup illustrated in Fig. 3 with the coordinate system

Preprints (www.preprints.org) | NOT PEER-REVIEWED | Posted: 6 April 2022 doi:10.20944/preprints202204.0038.v1

$$[Li^+] = Q_{Li}\exp(-2\beta\phi) \tag{A.3}$$

$$[Cl^-] = Q_{Cl}\exp(+2\beta\phi) \tag{A.4}$$

$$\phi \to 0 \quad (x \to +\infty) \tag{A.5}$$

Owing to the bulk phase electroneutrality, Eq. A.6 is derived by introducing Q_∞. Eqs. A.7 and A.8 are derived using Eqs. A.3 and A.4 by introducing $[Li^+]|_{x=0}$ $= Q^0_{Li}$, $[Cl^-]|_{x=0} = Q^0_{Cl}$ and $\phi|_{x=0} = \phi_0$.

$$Q_{Li} = Q_{Cl}(\equiv Q_\infty) \tag{A.6}$$

$$[Li^+]|_{x=0} = Q^0_{Li} = Q_\infty\exp(-2\beta\phi_0) \tag{A.7}$$

$$[Cl^-]|_{x=0} = Q^0_{Cl} = Q_\infty exp(+2\beta\phi_0) \tag{A.8}$$

Given that the solution charge density ρ in the left phase is represented by Eq. A.9, PB eq. for the experimental system in Fig. 3 is given by Eq. A.10.

$$\rho = eQ_\infty[\exp(-2\beta\phi) - \exp(+2\beta\phi)] \tag{A.9}$$

$$\frac{d^2\phi}{dx^2} = -\frac{\rho}{\epsilon\epsilon_o} = -\frac{eQ_\infty}{\epsilon\epsilon_o}[\exp(-2\beta\phi) - \exp(+2\beta\phi)] \tag{A.10}$$

Eqs. 5 and 11 are the boundary conditions for the potential.

$$\frac{d\phi}{dx} \to 0 \quad (x \to +\infty) \tag{A.11}$$

Using the electroneutrality for the entire left phase, Eq. A.12 holds where $\sigma|_{x=0}$ represents the charge density of lithium glass left surface.

$$\sigma|_{x=0} + \int_0^{+\infty} \rho dx \tag{A.12}$$

Eq. A.12 with respect to $\sigma|_{x=0}$ using Eqs. A.10 and A.11, Eq. A.13 is obtained.

$$\sigma|_{x=0} = 2\sqrt{2\epsilon\epsilon_o Q_\infty kT}\sinh(\beta\phi_0) \tag{A.13}$$

Preprints (www.preprints.org) | NOT PEER-REVIEWED | Posted: 6 April 2022 doi:10.20944/preprints202204.0038.v1

The total surface adsorption site density on the left surface of lithium glass is given by Eq. A.14.

$$[s]_T = [s] + [sLi^+] \tag{A.14}$$

Eq. A.15 is derived using Eqs. A.2 and A.14.

$$[sLi^+] = \frac{K_{Li}[s]_T[Li^+]|_{x=0}}{1 + K_{Li}[Li^+]|_{x=0}} \tag{A.15}$$

Eq. A.15 can be further arranged into Eq. A.16 using Eq. A.17.

$$[sLi^+] = \frac{K_{Li}[s]_T Q^0_{Li}}{1 + K_{Li}Q^0_{Li}} = \frac{K_{Li}[s]_T Q_\infty \exp(-2\beta\phi_0)}{1 + K_{Li}Q_\infty \exp(-2\beta\phi_0)} \tag{A.16}$$

$\sigma|_{x=0}$ can be represented by Eq. 17 and which should be same as Eq. A.13.

$$\sigma|_{x=0} = e[sLi^+] = \frac{eK_{Li}[s]_T Q_\infty \exp(-2\beta\phi_0)}{1 + K_{Li}Q_\infty \exp(-2\beta\phi_0)} \tag{A.17}$$

Owing to Eqs. A.13 and A.17, Eq. A.18 is derived, and it can be arranged into Eq. A.19.

$$\frac{eK_{Li}[s]_T Q_\infty \exp(-2\beta\phi_0)}{1 + K_{Li}Q_\infty \exp(-2\beta\phi_0)} = 2\sqrt{2\epsilon\epsilon_o Q_\infty kT}\sinh(\beta\phi_0) \tag{A.18}$$

$$\rightleftharpoons \quad \frac{eK_{Li}[s]_T \exp(-2\beta\phi_0)}{1 + K_{Li}Q_\infty \exp(-2\beta\phi_0)} = 2\sqrt{\frac{2\epsilon\epsilon_o kT}{Q_\infty}}\sinh(\beta\phi_0) \tag{A.19}$$

Experimentally given $[Li^+]|_{x=0}$ $(= Q_\infty)$ and the experimentally measured surface potentials of the lithium glass surface are summarized in Table 2. Plugging these experimental data into the RHS of Eq. A.19, Eq. A.19 was found to be constant as given by Eq. A.20.

$$2\sqrt{\frac{2\epsilon\epsilon_o kT}{Q_\infty}}\sinh(\beta\phi_0) \equiv M \sim const. \tag{A.20}$$

As long as Q_∞ is greater than 0.00001M, Eq. A.21 is valid. It can be easily confirmed by plugging the experimental data ϕ_0 into Eq. A.21.

$$\sinh(\beta\phi_0) \sim \frac{\exp(\beta\phi_0)}{2} \tag{A.21}$$

Solving Eq. A.20 using Eq. A.21 with respect to ϕ_0 results in Eq. A.21.

$$\phi_0 = N + \frac{2kT}{e}\ln\sqrt{Q_\infty} \qquad N \equiv \ const. \tag{A.22}$$

Eq. A.22 is rewritten as Eq. A.23 here.

$$\phi_0(\text{L(eft) phase}) \sim N + \frac{kT}{e}\ln Q^L_\infty \equiv \Phi^{ADS}_L \tag{A.23}$$

Preprints (www.preprints.org) | NOT PEER-REVIEWED | Posted: 6 April 2022 doi:10.20944/preprints202204.0038.v1

Appendix B

When z_i = -1, the key equation Eq. 18 turns into Eq. 11. Eq. 11 is originally Eq. 4. Eq. 4 was experimentally found to be constant regardless Q_∞. Then, it leads Eq. 8. Eq. 8. turns into Eq. B.1.

$$(K_{Cl}Q_{Cl} + K_{Br}Q_{Br})\exp(2\beta\phi_0) \sim A \tag{B.1}$$

Eq. B.1 could be be split into two terms as given by Eq. B.2 by introducing Eq. B.3. Therefore, Eq. B.1 may be interpreted as Eq. B.4.

$$\begin{aligned} & (K_{Cl}Q_{Cl} + K_{Br}Q_{Br})\exp(2\beta\phi_0) \sim A \\ \rightleftharpoons \quad & K_{Cl}Q_{Cl}\exp(2\beta\phi_0) + K_{Br}Q_{Br}\exp(2\beta\phi_0) \sim A_{Cl} + A_{Br} \end{aligned} \tag{B.2}$$

$$A \equiv A_{Cl} + A_{Br} \tag{B.3}$$

$$K_iQ_i\exp(2\beta\phi_0) \sim A_i \quad i \ = \ Cl^-, Br- \tag{B.4}$$

Eq. B.4 can be arranged into Eq. B.5. If A_ℓ can be defined by Eq. B.6, Eq. B.5 becomes Eq. B.7 and shows us its clear thermodynamical meaning. Eq. B.7 says that Eq. B.5 is the product of the binding constant K_ℓ and the concentration of ion i at the given position where the potential at the point is ϕ_0. And the authors believe Eq. B.7 "should" hold, otherwise, Eq. B.4 loses the thermodynamical meaning. Therefore, LHS of Eq. B.1 is merely the linear combination of Eq. B.8 which represents the Boltzmann disrtribution of mobile ions.

$$K_iQ_i \sim A_i\exp(-2\beta\phi_0) \tag{B.5}$$

$$A_i = K_iQ_{i\infty} \tag{B.6}$$

$$K_iQ_i \sim K_iQ_{i\infty}\exp(-2\beta\phi_0) \tag{B.7}$$

$$Q_i \sim Q_{i\infty}\exp(-2\beta\phi_0) \tag{B.8}$$

Now, let's forget so far discussed in **Appendix B** and let's focus on Eq. 2. By introducing Eq. B.9, Eq. 2 can be arranged into Eq. B.10.

$$\phi^{GHK} \equiv \Psi_L - \Psi_R \tag{B.9}$$

Preprints (www.preprints.org) | NOT PEER-REVIEWED | Posted: 6 April 2022 doi:10.20944/preprints202204.0038.v1

$$\begin{aligned} & \Psi_L - \frac{kT}{e}\ln(P_{Cl}[Cl]_L + P_{Br}[Br]_L) \\ = \; & \Psi_R - \frac{kT}{e}\ln(P_{Cl}[Cl]_R + P_{Br}[Br]_R) \quad (\text{where } [Br]_R = 0 \text{ M}) \end{aligned} \tag{B.10}$$

Since LHS and RHS of Eq. B.10 are independent each other, both of them should be constant. Hence, Eq. B.11 is derived.

$$(P_{Cl}[Cl]_j + P_{Br}[Br]_j)\exp(-2\beta\Psi_j) = B \quad B = \text{ const. } (j = L, R) \tag{B.11}$$

If P_j, Ψ_j and B can be redefined by Eqs. B.12, B.13 and B.14, respectively, it means that Eq. B.1 can be derived from the GHK eq., though Eq. B.1 is originally Eq. 8 which is founded on the ion adsorption mechanism [9,10].

$$P_j = K_j \tag{B.12}$$

$$\Psi_j = -\phi_j \text{ (Regard } \phi_0 \text{ of Eq. B.1 as } \phi_j) \tag{B.13}$$

$$B = A \tag{B.14}$$

So, even from the GHK eq. per se, we can reach Eq. B.11 which is same as Eq. B.1. And Eq. B.1 is originally Eq. 18 which is founded on the ion adsorption mechanism. Furthermore, it comes from the Boltzmann distribution of mobile ions.